

Binding energy of charged excitons in semiconductor quantum wells in the presence of longitudinal electric fields

Luis C. O. Dacal¹ and José A. Brum^{1,2}¹*IFGW-DFMC, Universidade Estadual de Campinas, C.P. 6165, 13083-970, Campinas-SP, Brazil*²*Laboratório Nacional de Luz Síncrotron - ABTLuS, C. P. 6192, 13084-971, Campinas-SP, Brazil*

(Received 27 September 2001; published 8 March 2002)

We present variational calculations of the binding energy for positively and negatively charged excitons (trions) in idealized GaAs/Al_{0.3}Ga_{0.7}As quantum wells with parabolic electrons and holes energy dispersions. The configuration interaction method is used with a physically meaningful single-particle basis set. We have shown that the inclusion of more than one electron quantum-well solution in the basis is important to obtain accurate values for the binding energies. The effects of longitudinal electric-field and quantum-well confinement on the charged excitons bound states are studied in the absence of magnetic field and the conditions for the trion ionization are discussed.

DOI: 10.1103/PhysRevB.65.115324

PACS number(s): 73.21.Fg, 78.67.De

I. INTRODUCTION

A quantum well (QW) is a layer of low-energy gap material grown between two others with larger gaps. This energy difference gives rise to electron and hole confinements in the lower gap material for type-I QW's. In this type of semiconductor heterostructure, optical transitions are dominated by Coulomb interactions.

In intrinsic QW's under low excitation power, when the same amounts of electrons and holes are present, the complex that dominates the photoluminescence spectrum is a neutral complex, the exciton, formed by the Coulomb interaction between one electron and one hole. On the other hand, in the case of a lightly modulation-doped QW, the charge excess makes it possible that the excitonic electrical dipole binds an extra carrier forming a charged complex (trion). In the case of a *p*-doped QW, the positive complex may be a bound state (X^+). This is analogous to the H_2^+ molecule in atomic physics. On the other hand, the negative complex (X^-) may be detected in *n*-doped structures, and is analogous to H^- . The stability of such charged complexes in semiconductors was first proposed by Lampert.¹

An interesting aspect of these complexes in semiconductor materials is that the magnetic fields available in laboratories produce strong effects on their binding energies. This creates a rich experimental situation that would only be possible in astrophysical systems for the cases of H^- and H_2^+ . Unfortunately, the calculated trion binding energy for semiconductor bulk materials² showed that its value is too low to be experimentally detected. However, this value is one order of magnitude larger in semiconductor quantum wells,³ as a consequence of the carriers confinement. This opened experimental possibilities in the case of high-quality samples.

The first experimental observation of a trion spectrum was made by Kheng *et al.*⁴ in a II-VI QW. In this case the trion binding energy is more than twice the value for III-V systems.⁵ Glasberg *et al.*⁶ investigated X^+ and X^- in the same sample, and showed that the binding energy of the negative trion singlet state increases faster than the positive one as a function of the magnetic field.

X^- was theoretically studied in the presence⁷⁻⁹ and in absence¹⁰ of a longitudinal magnetic field (applied along the growth direction) through different techniques. The *stochastic variational method*, with a basis set of *deformed correlated Gaussian functions*, was used by Riva *et al.*,⁸ and a good agreement with experiments was obtained. Whittaker and Shields⁹ worked with a Landau-level basis set for the in-plane (*xy*) motion, and showed the importance of including more than one QW level in the *z* (growth) direction wave-function component. In this case, the quasi-two-dimensional nature of the problem was explored, which was enhanced by the magnetic field applied parallel to the growth direction.

The X^- theoretical treatment is difficult. It is a few-body problem and, in our case, the low dimensionality has to be added to its complexity. Although the trion is a ground state, making it suitable for variational techniques, its stability can only be determined in comparison with its first excited state. Generally, this is an excitonic state with a noninteracting extra electron (hole) in the X^- (X^+) case, which is also variationally determined. As a consequence, it is rather complicated to determine the accuracy of the calculated trion binding energy.

Previous works did not succeed in presenting a detailed analysis of the exchange and correlation effects on the trion electronic structure. How the presence of the extra carrier affects the excitonic orbitals is an unclear question. To shed some light on this problem, we use the configuration interaction method¹¹ to build up a *physically clear* basis set and to calculate variational binding energies of positively and negatively charged excitons in idealized GaAs/Al_{0.3}Ga_{0.7}As quantum wells. We study the effects of the quantum-well confinement and longitudinal electric field on the charged exciton bound states in the absence of a magnetic field. Our basis allows us to have a good idea about the different contributions of the trion degrees of freedom to its binding energy.

II. MODEL

We consider a semiconductor QW, more exactly a GaAs layer between two Al_{0.3}Ga_{0.7}As layers treated within the ef-

fective mass and envelope function frameworks, considering z as the growth direction. The position $z=0$ is the quantum-well center, and we neglect the band bending due to the doping. This means that the electron and hole QW wave functions have well-defined parities. We also consider ideal QW interfaces, neglecting interdiffusion and doping potential fluctuations effects. The valence and conduction subbands are approximated by parabolic dispersions, which is more severe an approximation in the case of X^+ than in the case of X^- .

We start with the assumption that the QW confinement is strong enough to make a z and (x,y) separable wave function in the basis set reasonable. We use the noninteracting electron and hole QW solutions as the z part of the one-particle trial wave functions. When a longitudinal electric field (z axis) is present, the QW solutions are given by Airy functions,¹² which do not have well-defined parities. The continuum of states is simulated by a finite set of discrete states generated by a larger QW (1000 Å), with infinite barriers embedding the structure we are interested in.

The axial symmetry leads us to use polar coordinates to describe the X^- in-plane motion in terms of center of mass (CM) and relative to the hole coordinates:

$$\begin{aligned}\vec{\rho}_1 &= \vec{\rho}_{e1} - \vec{\rho}_h, \\ \vec{\rho}_2 &= \vec{\rho}_{e2} - \vec{\rho}_h, \\ \vec{\rho}_{CM} &= \frac{m_e(\vec{\rho}_{e1} + \vec{\rho}_{e2}) + m_{hxy}\vec{\rho}_h}{m_{hxy} + 2m_e},\end{aligned}\quad (1)$$

where the electron mass is isotropic. On the other hand, the hole dispersion is strongly nonparabolic in QW's, but, as a first approximation, the off-diagonal terms of the Luttinger Hamiltonian can be neglected. In this case, the hole mass is anisotropic, and shows a lighter in-plane value. In this approximation, the X^+ in-plane coordinates are easily obtained from the previous ones through the electron and hole label interchanges. We performed calculations for the negatively charged exciton binding energy using a QW-width-dependent in-plane mass for holes. This was made in the absence of external fields, and in the fundamental QW state approximation for holes. The maximum increase in the charged exciton binding energy (300-Å QW width) was less than 16%. As one can see, this mass dependency does not significantly change our quantitative results; therefore, it will be neglected. The negative trion CM mass is given by $m_{hxy} + 2m_e$. We use the same mass values for the well and barrier materials.

We label the trion states through the quantum numbers associated with the constants of motion, namely, the CM wave vector (K_{CM}), the z component of the total angular momentum ($M = m_1 + m_2$) and the total spin of the two electrons (X^-) or two holes (X^+) ($S = S_1 + S_2$).

The CM motion is uncoupled to the internal dynamics, and is described by a plane wave. Consequently, it will not be explicitly considered here. However, it is important to

note that, in the presence of a magnetic field, the CM and internal degrees of freedom are coupled since the trion is a charged complex.

The two electrons in X^- (holes in the case of X^+) are indistinguishable, and the configuration-interaction method is used to build up a nonorthogonal two-particle basis, in other words, we work with a basis set of Slater determinants and solve the *generalized eigenvalue problem*.

The spatial part of the charged exciton trial wave function with total relative particle angular momentum equal to M is given by

$$\begin{aligned}\Psi_{(m+n=M)} &= \sum_{i,j,m,n,p,q,r} c_{i,j,m,n,p,q,r} N_{i,j,m,n,p,q,r} \cdot \chi_p(z_h) \\ &\times [\chi_q(z_{e1}) \phi_i^m(\vec{\rho}_1) \chi_r(z_{e2}) \phi_j^n(\vec{\rho}_2) \\ &\pm \chi_r(z_{e1}) \phi_j^n(\vec{\rho}_1) \chi_q(z_{e2}) \phi_i^m(\vec{\rho}_2)],\end{aligned}\quad (2)$$

where $c_{i,j,m,n,p,q,r}$ is a linear variational parameter, $N_{i,j,m,n,p,q,r}$ is the determinant normalization, $\chi_q(z)$ is the q th electron (e) or hole (h) QW solution, and $\phi_i^m(\vec{\rho})$ is one relative particle wave function. The sum over the integer numbers m and n is restricted by the total relative particle angular momentum conservation: $M = m + n$. In Eq. (2), “+” builds up the singlet states, while “-” builds up the triplet ones. In the absence of magnetic field, only the singlet ($M=0$) is a bound state.

The in-plane relative particle wave function is given by

$$\phi_j^m(\vec{\rho}) = N_{j,m} \rho^m \exp\left[-\frac{\rho^2}{\lambda_j^2}\right] \exp[im\theta],\quad (3)$$

where $N_{j,m}$ is the relative particle function normalization, λ_j is an element of a set of physically meaningful parameters that determines the basis size, and m is an integer that defines the relative particle angular momentum. There is one set of λ parameters for each angular momentum. They are chosen through a geometric progression.¹³

The main advantages of the trial wave function, [Eq. (2)], rely on its analytical integration and its physical transparency. The relative particles are composed by one positive charge and one negative charge; therefore, we work with in-plane one particle functions that have the symmetry of two-dimensional atomic orbitals.

Analogously to the charged exciton case, the trial wave function of the neutral complex, the exciton, is given by

$$\psi_m = \sum_{i,j,k} c_{i,j,k} N_{i,j,k} \chi_i(z_h) \chi_j(z_e) \phi_k^m(\vec{\rho}),\quad (4)$$

where $\vec{\rho} = \vec{\rho}_e - \vec{\rho}_h$. In the following, we analyze the two different exciton complexes.

A. Exciton Hamiltonian

The exciton CM is a free particle, so we can omit its energy contribution. Using the relative coordinate for the in-plane motion, the exciton Hamiltonian is written as

$$H_{ex} = H(z_e) + H(z_h) + T_{xy} + V_c, \quad (5)$$

where

$$H(z_{e,h}) = -\frac{\hbar^2}{2m_{e,hz}} \frac{\partial^2}{\partial z_{e,h}^2} + V_{we,wh} Y\left(\frac{L}{2} - |z_{e,h}|\right) \pm |e|Fz_{e,h}, \quad (6)$$

$$T_{xy} = -\frac{\hbar^2}{2\mu} \left[\frac{1}{\rho} \frac{\partial}{\partial \rho} \left(\rho \frac{\partial}{\partial \rho} \right) + \frac{1}{\rho^2} \frac{\partial^2}{\partial \theta^2} \right], \quad (7)$$

$$V_c = -\frac{e^2}{\varepsilon \sqrt{(z_e - z_h)^2 + \rho^2}}. \quad (8)$$

Here the QW potential height for electrons (e) and holes (h) is given by $V_{we,wh}$, $Y(z)$ is the step function [$Y(z)=1$ if $z > 0$ and $Y(z)=0$ if $z < 0$], L is the QW width, F is the magnitude of the longitudinal electric field, μ is the exciton in-plane reduced mass, and $\varepsilon=13.2$ is the GaAs dielectric constant. The sign “+” is used for electrons, and “-” for holes, in the electric field component of $H(z_{e,h})$.

The relative particle angular momentum conservation assumes a simple form in the exciton case. The in-plane part of Eq. (5) is an effective one particle Hamiltonian, and the exciton ground-state basis set is built up with s -like functions. This means that m is a good quantum number and only $m=0$ terms have to be taken into account in Eq. (4).

We obtain good convergence for the exciton ground-state binding energy with seven lambda factors between 5 and 800 Å. The coupling of different conduction and valence QW subbands gives only marginal contributions to the energy.¹⁴ Despite this, we used a basis set with three (two) QW levels for electrons (holes), since they are necessary in the charged exciton case. The full basis set has 42 states.

B. Charged exciton Hamiltonian

Analogously to the exciton case, using the relative to the hole coordinates for the in-plane motion [Eq. (1)], the X^- Hamiltonian is given by

$$H_{ce} = \sum_{i=1,2} \{H(z_{ei}) + H(\vec{\rho}_i)\} + H(z_h) + \frac{1}{m_{hxy}} \vec{p}_1 \cdot \vec{p}_2 + \frac{e^2}{\varepsilon \sqrt{|\vec{\rho}_1 - \vec{\rho}_2|^2 + (z_{e1} - z_{e2})^2}}, \quad (9)$$

where

$$H(z_{ei,h}) = -\frac{\hbar^2}{2m_{ei,hz}} \frac{\partial^2}{\partial z_{ei,h}^2} + V_{we,wh} Y\left(\frac{L}{2} - |z_{ei,h}|\right) \pm |e|Fz_{ei,h}, \quad (10)$$

$$H(\vec{\rho}_i) = -\frac{\hbar^2}{2\mu} \left[\frac{1}{\rho_i} \frac{\partial}{\partial \rho_i} \left(\rho_i \frac{\partial}{\partial \rho_i} \right) + \frac{1}{\rho_i^2} \frac{\partial^2}{\partial \theta_i^2} \right] - \frac{e^2}{\varepsilon \sqrt{(z_{ei} - z_h)^2 + \rho_i^2}}. \quad (11)$$

Here \vec{p}_i is the in-plane linear momentum operator corresponding to the i th relative particle. The term proportional to $\vec{p}_1 \cdot \vec{p}_2$ is a consequence of our choice of coordinates transformation [Eq. (1)]. This term is inversely proportional to the hole mass, and it represents the hole mobility.¹⁵ The X^+ parabolic Hamiltonian is immediately obtained from Eq. (9) through an interchange of the electron and hole labels.

The charged exciton binding energy (E_b) is defined as the difference between the energy of this charged complex and the energy of an exciton (X^0), plus an in-plane free electron in the X^- case or a free hole in the X^+ case. Taking the ground-state energy of these carriers as zero, one can write

$$E_b(X^-/X^+) = E(X^-/X^+) - E(X^0). \quad (12)$$

It is important to emphasize that the charged exciton binding energy is a difference between two values obtained variationally. This means that the calculated trion binding energy is not necessarily an upper limit of the actual value.

III. RESULTS AND DISCUSSIONS

Since we are considering a GaAs/Al_{0.3}Ga_{0.7}As QW, the effective parameters used are $m_e=0.067m_0$, $m_{hz}=0.377m_0$, $m_{hxy}=0.112m_0$, and $\varepsilon=13.2$ for the well and barrier materials. The conduction (valence) band offset is 224.5 meV (149.6 meV).

Our results show that, in the absence of magnetic fields, there is only one bound state, the singlet $M=0$. This is in agreement with previous calculations.¹⁰

In Fig. 1 we show the binding energy of the X^- singlet ($M=0$) state, $E_b(X^-)$, as a function of the QW width for different levels of approximation. In all of them only the fundamental QW states are taken into account. The most important contribution is given by the s -like relative particle state (dashed line). We obtain an excellent convergence for eight values of the λ parameter (between 50 and 800 Å), which means a basis set with 36 Slater determinants (squares). The results show the expected behavior with larger binding energies for the narrowest QW's. The highest value is reached for $L \sim 30$ Å, where the charge confinement is maximum. For comparison we also show the results obtained using just one λ value for each relative particle function in which case they are the variational parameters (dashed line). Adding the higher relative particle angular momenta to the basis set, but keeping $M=0$, we observe a binding-energy increase of the order of 50%.

Let us first analyze the cases in which the term $+(1/m_{hxy})\vec{p}_1 \cdot \vec{p}_2$ is neglected [Eq. (9)]. Note that this term has no contribution when only s states are considered. The most important contribution of the nonzero angular momentum wave functions is related to the repulsive Coulomb in-

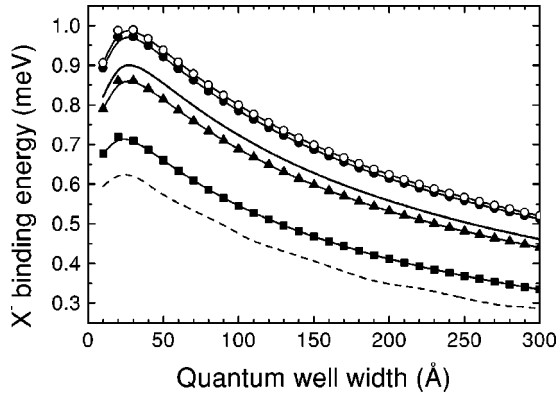


FIG. 1. X^- binding energy as a function of the QW width for different degrees of approximation: only s states and one λ value for each relative particle function (dashed line); only s states but with a set of eight values of λ (squares); the same as before but including the p^\pm -state contribution (triangles); full calculation including the d^\pm -state contribution (full line). The two upper curves are equivalent to the last two, but neglecting the $+(1/m_{hxy})\vec{p}_1 \cdot \vec{p}_2$ term (open circles include up to the d states, while solid circles include only the s and p states).

teraction. The s states favor the electrons being closer to the hole, while the other ones favor the electrons being far from each other. Although these contributions are important, we obtain a good convergence adding only the p^\pm and d^\pm states to the basis set (solid and open circles, respectively). Finally, when we add the repulsive $+(1/m_{hxy})\vec{p}_1 \cdot \vec{p}_2$ term, a binding-energy decrease of the order of 10% is observed. However, this does not change the fact that a basis with only s , p^\pm and d^\pm states is sufficient to obtain a convergence in the binding energy (triangles and full line respectively).

Figure 2(a) shows charged exciton binding energies obtained with different numbers of QW states in the basis set. In the case of X^- , what will be called full results take into account two hole QW states and three electron QW states which are enough to obtain a good convergence. The results with two electronic subbands present a discontinuity at 50 Å. At this width, the second QW solution for electrons becomes a QW bound state. As a result, there is an oscillator strength redistribution between the states inside and outside the QW. If an extra electron level is included in the basis, this discontinuity is smoothed out. However, one can see that another discontinuity appears when the third QW solution for electrons becomes a bound state inside the well (100 Å). When a larger number of QW states is used, these discontinuities are completely smoothed out. This raises the numerical calculation efforts without a significant improvement of our results. The X^+ results are equivalent, and only the full results are shown using two electron QW states and three hole ones (circles). As one can see in Fig. 2, the excited QW levels are important to describe the charged exciton fundamental state.

The main reasons for including more than one electron QW level in the charged exciton basis are the correlation and exchange effects. The QW hole subbands are energetically nearer than the electronic ones, favoring their coupling mainly for wide QW's. This effect can be noted in Fig. 2(a). The inclusion of the second QW even solution for holes

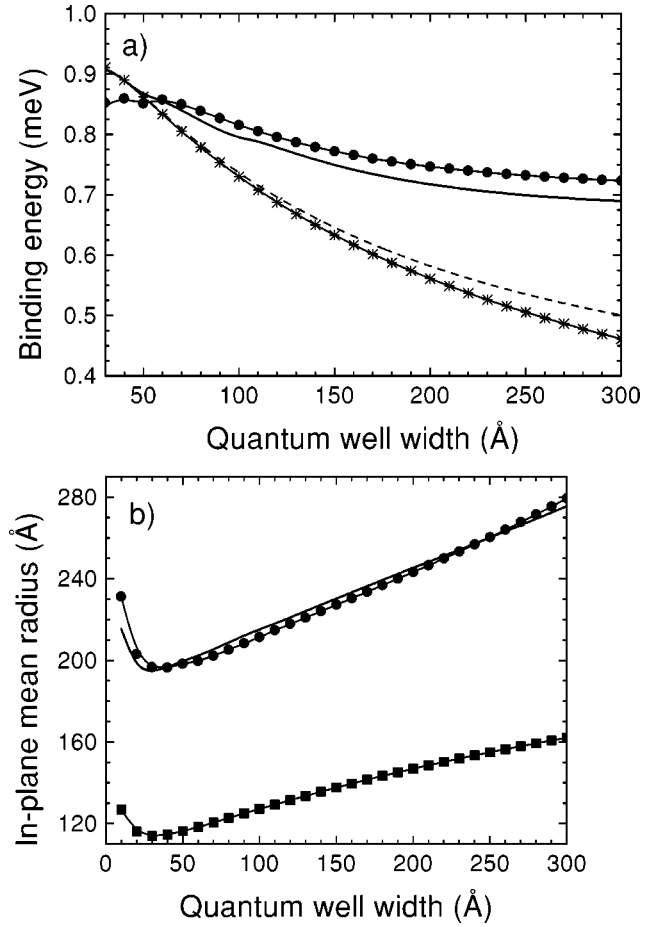


FIG. 2. (a) Charged exciton binding energy as a function of the QW width. The X^- values were calculated using one-electron and one-hole subbands (stars), one-electron and two-hole subbands (dashed line), and three-electron and two-hole subbands (full line). The X^+ results (circles) were obtained using three-hole and two-electron subbands. (b) Mean value of the in-plane relative particle radius for the exciton (squares), X^- (full line), and X^+ (circles) calculated with the complete basis.

gives rise to a binding energy gain of the order of 9% for the largest quantum well. The electron contributions are more delicate: in the exciton case, the electron QW ground state already gives us the binding energy convergence. However, this is not the case for X^- . The particle interchange symmetry requires a flexible basis which cannot be limited to the fundamental electron QW state. In the case of a 300-Å quantum-well width, the full calculation increases the X^- binding energy by 40%, compared with the case where two hole QW levels and only one electron QW level are taken into account. Nevertheless, there are two aspects that should be pointed out. One is that if more than one electron QW level is considered, the coupling between the even and odd QW solutions is allowed. The other is that the exciton binding energy is almost one order of magnitude larger than the charged exciton one.

One can see in Fig. 2(a) that as the QW becomes wider, the charged exciton becomes more weakly bound due to the effective one-dimensional confinement decrease. The heavy hole is more localized by the quantum-well potential than the

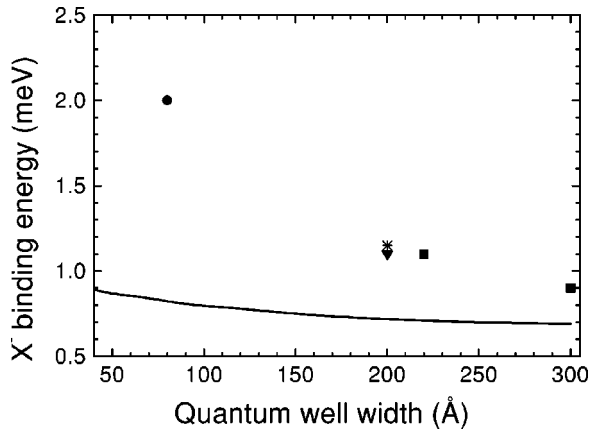


FIG. 3. X^- binding energy as a function of the QW width. The solid line corresponds to our full calculation. The points are experimental data from Ref. 6 (down triangle), Ref. 16 (star), Ref. 17 (circle), and Ref. 18 (squares).

electrons. Because of this, for QW widths less than 60 Å the strong overlap between the two holes of the X^+ enhances the Coulomb repulsion and the positively charged exciton is less bound than the negative one. For wider QW's, the less effective confinement and the hole subband coupling lead the X^+ and X^- to present similar binding energies. This is in agreement with the experimental results of Glasberg *et al.*⁶ and Finkelstein *et al.*¹⁶

Figure 2(b) shows the mean value of the in-plane relative particle radius for X^- (full line), X^+ (circles), and excitons (squares). As expected, the lower the binding energy of the complex, the larger its in-plane relative particle radius. These values should be compared to the exciton ones, which present a much smaller complex.

We compare our results with experimental ones in Fig. 3. Although the calculated binding energies are always lower than the experimental ones, it is important to realize that in the wide QW limit they are in good agreement. It is known that the sample structural defects increase the charged exciton binding energy, and that they are less important for wide QWs where the wave-function amplitudes are lower at the interfaces. Therefore, we attribute the results discrepancy to the effects of interface defects (Riva *et al.*¹⁰).

Most of the samples where the trions have been observed are one-side modulation doped. This is made in order to improve the optical characteristics of the QW. As a consequence, they have a built-in electric field along the growth direction. To obtain a clearer idea about this effect on the trion binding energy, we considered the presence of an electric field applied along the z direction. In Fig. 4, we show the X^- binding energy (a) and the in-plane mean radius (b) as functions of the longitudinal electric field. Three QW widths are considered: 100 Å (solid line), 200 Å (stars), and 300 Å (dashed line). Our results are in good agreement with the theoretical values obtained by Esser *et al.*¹⁹ The charge confinement is stronger for the narrowest well. In this case, the electric-field effects are weaker. It is interesting to observe that the X^- binding energy increases slightly for fields up to 10 kV/cm. In Fig. 4(a), this is clearer for the 100-Å QW (solid line). At higher values of electric field, the carrier

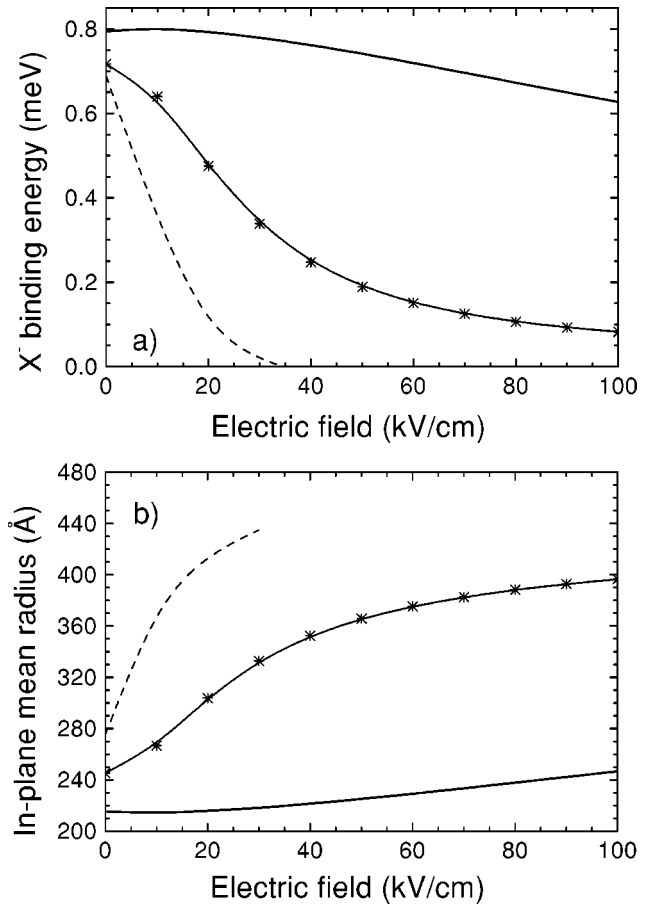


FIG. 4. (a) X^- binding energy as a function of longitudinal electric field for a 100-Å QW width (solid line), 200-Å QW width (stars) and 300-Å QW width (dashed line); (b) mean value of the in-plane relative particle radius.

wave functions begin to be localized at opposite QW interfaces. This phenomenon enhances the Coulomb repulsion at the same time that the attraction is weakened. For larger QW's, the electric field has a more important contribution, and the X^- binding energy decreases quickly. In this situation, the confinement is less effective and the carriers are more easily localized at opposite QW interfaces. As a consequence, an initial X^- binding-energy increase is observed at lower electric fields for 200- and 300-Å QW widths (see Fig. 5). For a 300-Å quantum-well width X^- becomes unbound for electric fields higher than 30 kV/cm, a result not observed for excitons under similar conditions.²⁰ Nevertheless, this result has to be understood as a limitation of our basis set [Eq. (2)], which is not able to reproduce the X^- continuum (an excitation plus an in-plane free electron). In fact, this “unbound” state means that the binding energy is not sufficiently high to be experimentally detected. The X^+ has the same qualitative behaviors (not shown), but it becomes “unbound” only for electric fields higher than 40 kV/cm in the case of a 300-Å QW width. It is important to remind the reader that, in all cases, the trion is an unbound state since, in the presence of longitudinal electric fields, the QW does not hold any carrier bound state in the strict sense. However, just as in the exciton case, QW's present strong resonances with

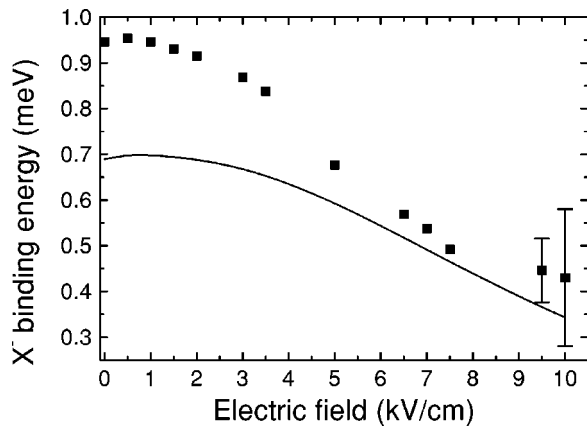


FIG. 5. X^- binding energy as a function of longitudinal electric field for a 300-Å quantum-well width. The solid line corresponds to our full calculation. The squares are experimental data from Ref. 21. The experimental error bars are shown for the two last points. At lower electric-field values, the error bars are not significant.

a long lifetime enabling their optical detection. Figure 4(b) shows that, as a general trend, the relative particle coordinates increase their average values for higher electric fields. It is also interesting to note that the initial binding-energy increase for the 100-Å QW is accompanied by a slight relative particle radius reduction. In actual samples, the in-built electric field is rather small.

Figure 5 shows a comparison between our results and the experimental data from Shields *et al.*²¹ One can see that the agreement is better for higher electric-field values when the

positive and negative carriers are more spatially separated and the repulsion dominates over the attraction. It is known that the QW interfaces do not possess the same quality during the growth process. The longitudinal electric field pushes the electrons, which are more sensitive to interface defects, toward the *good* interface. Consequently, the good agreement at higher electric-field values may indicate again that the main reason for the experimental and theoretical results discrepancy is the presence of structural imperfections. Another interesting point is the experimental observation of the slight X^- binding-energy increase for low electric-field values. This shows that our approximations retains the most important physical characteristics of the complex.

IV. CONCLUSION

In conclusion, we variationally calculated the trion binding energy in GaAs/Al_{0.3}Ga_{0.7}As semiconductor QW's. We showed that a flexible trial wave function, including the z -related degree of freedom, is required to obtain accurate results. In the presence of a longitudinal electric field, we observe very low trion binding energies for wide QW's. We believe that the interface defects have an important role in the trion dynamics, especially in the narrow QW and low-field limits.

ACKNOWLEDGMENTS

This work was supported by FAPESP (Brazil) and CNPq (Brazil).

- ¹M. A. Lampert, Phys. Rev. Lett. **1**, 450 (1958).
- ²G. Munschy and B. Stébé, Phys. Status Solidi B **64**, 213 (1974).
- ³B. Stébé and A. Ainane, Superlattices Microstruct. **5**, 545 (1989).
- ⁴K. Kheng, R. T. Cox, Y. Merle d'Aubigné, Franck Bassani, K. Saminadayar, and S. Tatarenko, Phys. Rev. Lett. **71**, 1752 (1993).
- ⁵G. Finkelstein, V. Umansky, I. Bar-Joseph, V. Ciulin, S. Haacke, J. -D. Ganiere, and B. Deveaud, Phys. Rev. B **58**, 12 637 (1998).
- ⁶Shmuel Glasberg, Gleb Finkelstein, Hadas Shtrikman, and Israel Bar-Joseph, Phys. Rev. B **59**, R10 425 (1999).
- ⁷A. B. Dzyubenko and A. Yu. Sivachenko, Phys. Rev. Lett. **84**, 4429 (2000).
- ⁸C. Riva, F. M. Peeters, and K. Varga, Phys. Rev. B **63**, 115302 (2001).
- ⁹D. M. Whittaker and A. J. Shields, Phys. Rev. B **56**, 15 185 (1997).
- ¹⁰C. Riva, F. M. Peeters, and K. Varga, Phys. Rev. B **61**, 13 873 (2000).
- ¹¹R. McWeeny and B. T. Sutcliffe, *Methods of Molecular Quantum Mechanics* (Academic Press, London, 1969).
- ¹²J. A. Brum, C. Priester, and G. Allan, Phys. Rev. B **32**, 2378 (1985).
- ¹³C. Aldrich and R. L. Greene, Phys. Status Solidi B **93**, 343 (1979).
- ¹⁴C. Priester, G. Bastard, G. Allan, and M. Lannoo, Phys. Rev. B **30**, 6029 (1984).
- ¹⁵J. A. Brum and P. Hawrylak, Comments Condens. Matter Phys. **18**, 135 (1997).
- ¹⁶G. Finkelstein, H. Shtrikman, and I. Bar-Joseph, Phys. Rev. B **53**, R1709 (1996).
- ¹⁷Z. C. Yan, E. Goovaerts, C. Van Hoof, A. Bouwen, and G. Borghs, Phys. Rev. B **52**, 5907 (1995).
- ¹⁸A. J. Shields, M. Pepper, D. A. Ritchie, M. Y. Simmons, and G. A. C. Jones, Phys. Rev. B **51**, 18 049 (1995).
- ¹⁹A. Esser, E. Runge, R. Zimmermann, and W. Langbein, Phys. Status Solidi B **221**, 281 (2000).
- ²⁰J. A. Brum and G. Bastard, Phys. Rev. B **31**, 3893 (1985).
- ²¹A. J. Shields, F. M. Bolton, M. Y. Simmons, M. Pepper, and D. A. Ritchie, Phys. Rev. B **55**, R1970 (1997).